

# Remote mid-infrared sensing using Chirped Laser Dispersion Spectroscopy

Michal Nikodem<sup>\*a</sup>, Clinton Smith<sup>a</sup>, Damien Weidmann<sup>b</sup>, Gerard Wysocki<sup>\*\*a</sup>

<sup>a</sup>Electrical Engineering Department, Princeton University, Princeton, NJ, 08544, USA

<sup>b</sup>Space Science and Technology Department, STFC Rutherford Appleton Laboratory, Didcot, Oxfordshire, OX11 0QX, UK

\*mnikodem@princeton.edu; \*\*gwysocki@princeton.edu; phone: 609-258-8187.

## ABSTRACT

A new spectroscopic technique for remote molecular detection is presented. Chirped Laser Dispersion Spectroscopy (CLaDS) uses a two-color dynamic interferometric heterodyne detection to measure optical dispersion caused by molecular transitions. The dispersion sensing is based on measurement of instantaneous frequency of an optical heterodyne beatnote which provides high immunity to optical power fluctuations. Thus CLaDS is well suited to long distance remote sensing and open-path monitoring. In this work we present CLaDS experimental setup for remote sensing of nitric oxide using 5.2  $\mu\text{m}$  quantum cascade laser. System performance as well as advantages and limitations are discussed.

**Keywords:** spectroscopy, dispersion spectroscopy, CLaDS, mid-infrared spectroscopy, optical heterodyning, gas sensing, nitric oxide, quantum cascade laser

## 1. INTRODUCTION

Laser technology offers unique capabilities that allow for remote, non-invasive chemical sensing. The invention of quantum cascade lasers (QCLs), which are compact semiconductor laser sources, allowed for development of small footprint instrumentation that can access the strongest fundamental molecular absorption bands in the mid-infrared between 3 and 12  $\mu\text{m}$  [1]. Access to this spectral region enables ultra-sensitive concentration measurements with minimum detection limits ranging from part-per-million by volume (ppmv) down to parts-per-trillion by volume (pptv) depending on target molecules and detection methods used [2]. In the last decade a significant progress in mid-IR technology has led to transfer of the QCL-based sensors from laboratories to the field.

While QCL-based single-point, extractive sensors have been extensively studied [3, 4] and are becoming available commercially [5, 6], remote sensing with QCLs has been limited to basic studies in a direct laser absorption spectroscopy configuration [7]. Thus new technologies with higher immunity to returned optical power fluctuations are needed to enable longer distances and applications of topographic targets in place of retro-reflectors. This can be realized when molecular sensing is based on phase-related dispersion measurements instead of absorption sensing, which relies on intensity detection.

In this paper we present a chirped laser dispersion spectroscopy (CLaDS) technique [8] for remote detection of chemical species. CLaDS is based on detection of the optical dispersion associated with the target molecular transitions. This makes it suitable for remote trace-gas detection in environments with large transmission fluctuations. In the following sections a theoretical background of CLaDS, the signal and noise performance as well as examples of ultrasensitive detection of nitric oxide (NO) are presented.

## 2. CLaDS - THEORY

Interaction of light with matter in the vicinity of an optical resonant transition of the irradiated medium results in absorption and dispersion of the transmitted light wave. For a given sample, knowledge of the frequency dependence of the absorption coefficient allows the evaluation of the dispersion via the Kramers-Kronig transformation, which relates the refractive index  $n(\omega)$  and the absorption coefficient  $\alpha(\omega)$  of a sample as:

$$n(\omega) = 1 + \frac{c}{\pi} \int_0^{\infty} \frac{\alpha(\omega')}{\omega'^2 - \omega^2} d\omega', \quad (1)$$

where  $c$  is the speed of light and  $\omega$  the optical angular frequency.

Molecular sensing using dispersion measurement is more challenging than probing the absorption, but it also presents important advantages. For example commonly used gas detection methods such as direct absorption measurements or wavelength modulation spectroscopy (WMS) are sensitive to changes of the optical power that arrives to the detector. In contrast, if we analyze dispersion by detecting the phase of the light, intensity independent measurement can be realized. This feature is particularly important in open-path remote sensing application where the amount of light that reaches the photodetector can strongly fluctuate due to transmission variations or turbulence.

In this paper we present a chirped laser dispersion spectroscopy (CLaDS) system adopted for remote molecular sensing applications. The arrangement of the optical system used to demonstrate this technique is shown in Fig. 1a. A beam from a frequency-chirped QCL is divided into two frequency-shifted beams using an acousto-optical modulator (AOM). The 0th and the 1st order fields can be expressed as two electromagnetic waves:

$$E_1 = A_1 \cos(\omega_1 t - \varphi_1), \quad (2a)$$

$$E_2 = A_2 \cos(\omega_2 t - \varphi_2), \quad (2b)$$

with  $A$ ,  $\omega$ , and  $\varphi$  being the amplitude, the optical angular frequency, and the phase of the two fields, respectively. The two fields are recombined into one dual-frequency beam using a Mach-Zehnder interferometer arrangement. When the fields are overlapped at the detector plane, a photocurrent produced is proportional to:

$$I_{ph} \propto A_1^2 + A_2^2 + 2A_1A_2 \cos[(\omega_1 - \omega_2)t - (\varphi_1 - \varphi_2)] = A_1^2 + A_2^2 + 2A_1A_2 \cos(\phi), \quad (3)$$

where the third term is the time-dependent beat term oscillating at the difference frequency  $\Omega = \omega_1 - \omega_2$ . Assuming that the instantaneous optical angular frequency of a laser is linearly chirped with the chirp rate  $S$ , it can be expressed as:

$$\omega(t) = \omega_0 + St. \quad (4)$$

By taking it into account and by introducing an additional phase shift acquired during the propagation through the optical system the two fields can be expressed as:

$$E_1 = A_1 \cos \left[ \omega_0 \cdot (t - \Delta t_1) + \frac{1}{2} S \cdot (t - \Delta t_1)^2 \right], \quad (5a)$$

$$E_2 = A_2 \cos \left[ \omega_0 \cdot (t - \Delta t_2) + \frac{1}{2} S \cdot (t - \Delta t_2)^2 - \Omega \cdot (t - \Delta t_2) \right] \quad (5b)$$

where  $\Delta t_1$  and  $\Delta t_2$  are times required for each wave-front to reach the detector plane. The time dependent phase of the RF beatnote becomes:

$$\phi(t) = [\Omega + S \cdot (\Delta t_2 - \Delta t_1)]t - \Omega \Delta t_2 + \omega_0 \cdot (\Delta t_2 - \Delta t_1) - \frac{1}{2} S \cdot (\Delta t_2^2 - \Delta t_1^2). \quad (6)$$

By applying frequency demodulation the instantaneous frequency of the RF beatnote  $f(t) = \frac{1}{2\pi} \frac{d\phi}{dt}$  can be determined. This instantaneous frequency can also be expressed as a function of the optical frequency as:

$$f(\omega) = \frac{1}{2\pi} \left\{ \Omega + \frac{S \cdot \Delta L}{c} - \frac{S L_C}{c} \cdot \omega \cdot \left( \frac{dn}{d\omega} \Big|_{\omega - \Omega} - \frac{dn}{d\omega} \Big|_{\omega} \right) \right\}, \quad (7)$$

where  $\Delta L$  is the path length difference between the two interferometer arms,  $L_C$  is the total optical path length within the sample and  $n$  is the refractive index. Equation 7 shows that the RF beatnote at the carrier frequency  $\Omega$  contains information about the optical path difference  $\Delta L$  as well as about the dispersion occurring along the optical path length  $L_C$ . When  $\Delta L$  is set to zero the frequency demodulation of the RF beatnote at the frequency  $\Omega$  provides a baseline-free signal, which is additionally enhanced by the chirp rate  $S$  and by the optical frequency  $\omega$ . More importantly, the dispersion signal does not depend on the amplitude of the heterodyne beatnote, and hence is strongly immune to changes in the optical power that reaches the detector. Additionally the dispersion exhibits linear dependence on the concentration of the target species, which allows for a large dynamic range of concentration measurements without affecting the actual precision of the instrument. Figure 1b shows the simulation of the peak absorption and the peak dispersion signal for NO transition at  $1906.7 \text{ cm}^{-1}$  for concentrations between 0.025 and 0.5 % of NO in  $\text{N}_2$  mixture. When detecting high concentration samples (or by increasing the optical path) the Beer-Lambert law becomes non-linear

and small changes in concentration can no longer be measured. This limits the achievable accuracy for high sample concentrations using conventional absorption methods. In contrast, the peak amplitude of the dispersion signal is proportional to the concentration throughout the entire range of sample transmission. This feature is particularly important in long-distance mid-IR sensing when path-integrated absorption may be relatively high.

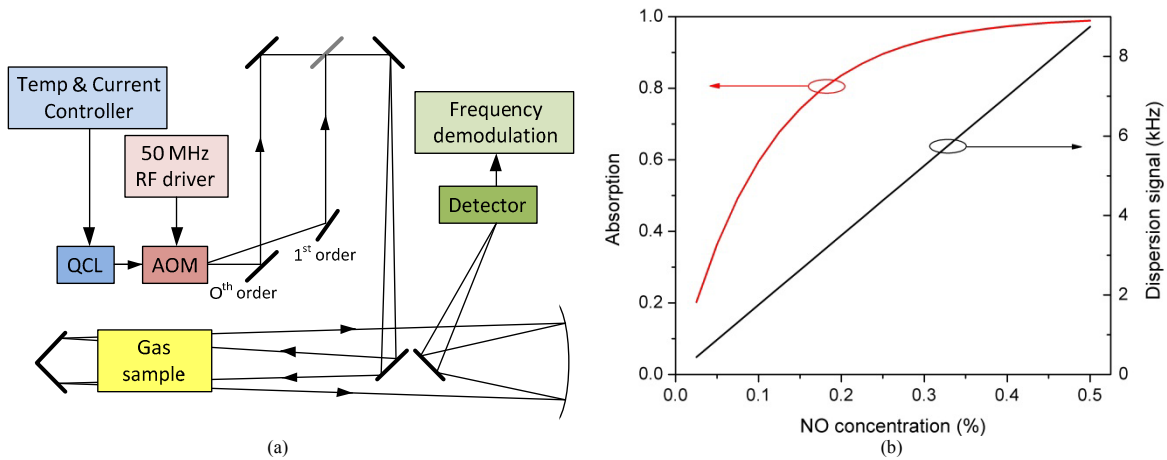


Figure 1. (a) A diagram of an experimental set-up; (b) peak absorption and dispersion signals calculated using HITRAN database for NO transition at  $1906.7 \text{ cm}^{-1}$  as a function of sample concentration (pressure = 760 Torr, chirp rate  $S = 0.5 \text{ MHz/ns}$  and path length = 1 m).

### 3. Remote CLaDS - EXPERIMENT

A continuous wave  $5.2 \mu\text{m}$  distributed feedback QCL was used in the experiment. The QCL optical frequency was chirped quasi-linearly by applying a triangular modulation of the injection current. The two frequency-shifted beams generated by a germanium AOM driven with a 50 MHz signal were recombined into one and directed towards a retro-reflector. A gas cell filled with the NO/N<sub>2</sub> mixture was used as a sample. The cell was placed in front of the retro-reflector, approximately 10 m away from the system. The returning light was collected with a telescope and focused onto a fast thermoelectrically cooled mercury cadmium telluride photodetector. An RF spectrum analyzer was used to perform frequency demodulation of the RF beatnote.

#### 3.1 Amplitude of the CLaDS molecular dispersion signal

The CLaDS molecular dispersion signal produced in the vicinity of the molecular transition is described by Eq. 7. The amplitude of this signal is proportional to the chirp rate  $S$ , which is especially significant when QCLs that can exhibit high frequency chirp rates are used [3]. In order to demonstrate how the amplitude of the dispersion signal depends on the chirp rate we varied the frequency of the triangular QCL current modulation added to the QCL bias current. By creating a small well defined path difference in the interferometer ( $\Delta L$  in Eq. 7) we were able to precisely determine the chirp rate for each measurement before the sample gas cell was placed within the optical path. The laser wavelength was tuned to target an NO doublet around  $1906 \text{ cm}^{-1}$  and a peak-to-peak value of the dispersion signal amplitude in the spectrum was measured. A 12.5 cm-long cell was filled with 0.8% of NO, 99.2% of N<sub>2</sub> at a total pressure of 5 Torr.

Figure 2 shows the results after averaging 500 consecutive scans for chirp rates between 20 kHz/ns and 1325 kHz/ns. Signals for the smallest and the largest chirp rate used are presented in Fig. 2a; whereas Fig. 2b shows the linear fit of the dispersion signal amplitude vs. chirp rate. Fig. 2a clearly shows that if the acquisition parameters (such as acquisition bandwidth, FM detection bandwidth, *etc.*) are adjusted accordingly, the change in the scanning rate does not affect the spectral shape of the dispersion line and only enhances the signal amplitude. The experimental data show a well-defined linear dependence and are in excellent agreement with the theoretical predictions based on Eq. 7.

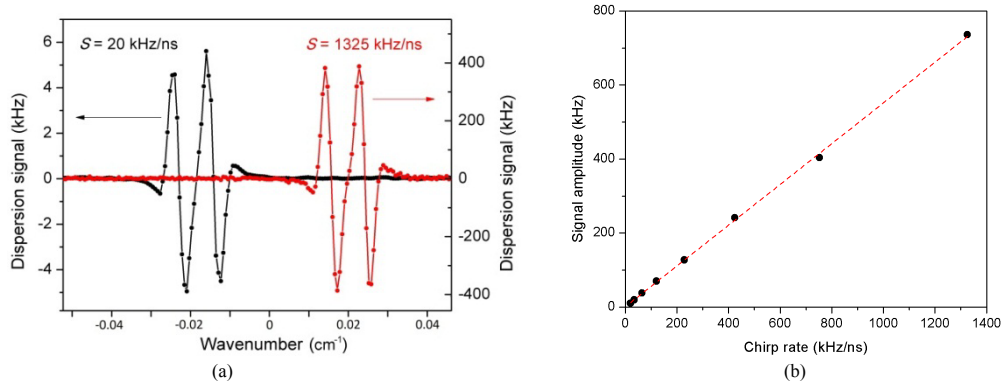


Figure 2. (a) Dispersion signal measured for the fastest and the slowest chirp rate; (b) amplitude of the dispersion signal vs. chirp rate. Measured data (black dots) show linear dependence (red line –linear fit with  $R^2 = 0.9995$ ).

Based on these observations the CLaDS measurement process is primarily limited by two factors:

- The maximum chirp rate may be limited by the laser source itself or by a finite bandwidth of the laser current controller,
- High chirp rates require wider bandwidth hence the chirp rate is limited by the frequency shift of the AOM (the bandwidth of CLaDS signal should be smaller than carrier frequency) and by the maximum bandwidth of the frequency demodulator.

### 3.2 Noise performance in CLaDS

Although increasing scanning speed results in higher amplitude of the CLaDS signal, the signal to noise ratio (SNR) shows a significantly more complex relationship. The reason is that the noise in CLaDS is also affected by the chirp rate both in a direct and an indirect way. A direct impact of the chirp rate on the noise is through ‘fringe noise’ caused by the presence of unwanted interferences that result in parasitic fringe signal. In our system the broadband antireflective coatings on the AOM are unable to fully prevent the formation of the etalon between the front and back facets of the AOM. A Fabry-Perot cavity affects both the intensity and phase of the light, thus it produces fringes also in the dispersion signal measured by CLaDS. If the fringe pattern contains features comparable to the target absorption lines it becomes hard to distinguish and thus it should be considered as noise. The indirect impact of the chirp rate on the total noise in CLaDS is related to the effective bandwidth of the dispersion signal. Faster chirp rates cause the bandwidth of the modulating dispersion signal to increase, which in effect requires larger demodulation bandwidth  $BW$ . The theory of FM-modulation clearly shows that noise at the output of an FM-demodulator grows as  $BW^2$  [9], thus it must be taken into account especially at higher chirp rates. We also observed an instrumental noise contribution that is independent of the chirp rate. This noise is concentrated at low frequencies and the origin of this noise requires further investigation. However, for any practical acquisition bandwidths it can be considered as a constant random noise contribution within the total noise observed.

In order to evaluate the noise performance of the CLaDS system we have analyzed how the noise level depends on the chirp rate. Figure 2b shows a linear dependence of the CLaDS signal amplitude vs. chirp rate that was calculated based on a set of measurement results. The same experimental data is used to find how the noise depends on the chirp rate. For this analysis we define the noise as standard deviation of the CLaDS signal measured away from the molecular transition. Results are shown in Fig. 3a. For each measurement point the demodulation bandwidth  $BW$  was adjusted to keep the  $BW/S$  ratio constant, which assures sufficient bandwidth for the signal demodulation and results in the same RF spectral resolution.

Since the origins of the noise components are different we have fitted the data with the function  $N = f(S) = ((A \cdot S^2)^2 + C^2)^{0.5} + B \cdot S$ , where A, B and C are the coefficients that describe the contribution of, the demodulation noise, the fringe noise and the constant instrumental noise contribution, respectively. The fitting yields  $A=0.63e-3$ ,  $B=67.6e-2$  and  $C=13.8$  and shows excellent agreement between the data and the proposed model. Additional measurements in which only one parameter (chirp rate  $S$  or demodulation bandwidth  $BW$ ) was being changed while the other was kept constant confirmed that fringe noise and demodulation bandwidth change (which is proportional to  $S$ ) are responsible for the linear and the quadratic contribution respectively. The coefficients A, B and C clearly show that in the presented setup total noise is dominated by fringes.

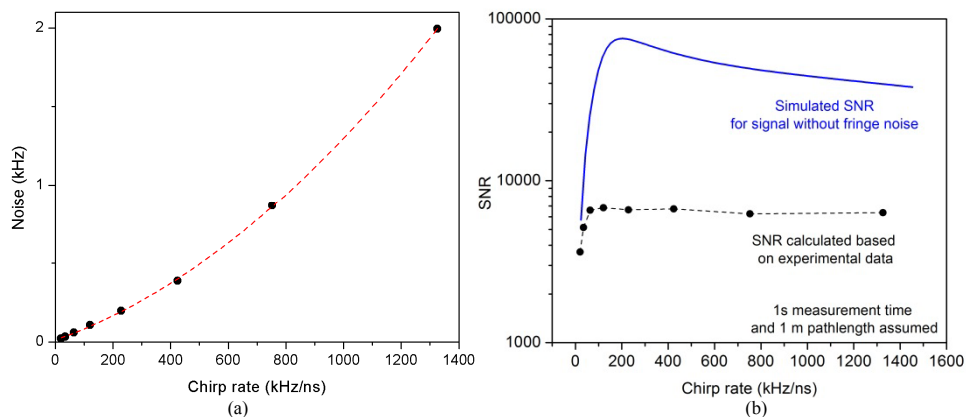


Figure 3. (a) Noise measured as a standard deviation of the dispersion signal away from the molecular transition vs. chirp rate. Acquisition bandwidth was adjusted for each scanning speed to minimize noise associated with frequency demodulation. Polynomial fit is shown; (b) SNR for measured data (black) and SNR calculated assuming fringe noise is removed (blue). Both extrapolated to 1 m pathlength and 1 s averaging time.

Figure 3b shows the calculated SNR for the measured data after extrapolation to the integration time of 1 second. However, such a simple extrapolation assumes that noise is purely Gaussian. Unfortunately, fringe noise is not random and cannot be approximated this way, but such an approach gives an ultimate SNR limit in case the fringe noise is also reduced. Based on the previously determined coefficients A, B and C we can calculate the ultimate SNR. As shown in Fig. 3b the SNR calculated this way suggests that with fringe reduction it should be possible to increase the SNR by one order of magnitude. It also shows that for the optimum chirp rate an SNR of more than 75000 can be expected, which corresponds to a minimum detection limit of 0.1 ppm for 1 m pathlength and 1 s averaging time.

#### Optical fringe reduction

If the optical interfaces that contribute to fringe formation have been identified a simple way to remove fringe noise is by varying the etalon length while averaging the measurement results. This method is usually realized by putting one of the elements that forms the unwanted cavity on a piezo-controlled stage to modulate the length of the etalon [10]. In the present setup fringes are generated within the AOM and the only way to change its optical length is by changing its operating temperature (etalon tuning through thermal expansion or refractive index change). This method enables significant improvement of the SNR in our system. Figure 4 shows two spectra: one acquired in stable conditions and one acquired after temperature of the AOM was varied. The concentration of the NO for this measurement was reduced to approximately 0.1% NO in N<sub>2</sub> and the pressure was set to ~10 Torr. The wavelength of the laser was tuned to target the transition at 1906.7 cm<sup>-1</sup>. In both measurements the chirp rate was set to 420 kHz/ns and 10000 scans at 25 kHz repetition rate were averaged (with a total acquisition time of 400 ms). The demodulation bandwidth was set to  $BW = 5$  MHz to assure sufficient number of measurement points for accurate data fitting.

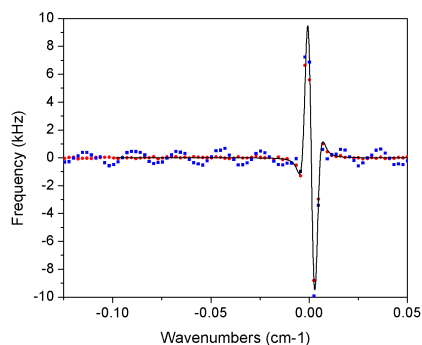


Figure 4. Dispersion signal measured in stable conditions (blue dots) and when temperature of the AOM was varied during data acquisition (red dots). Significant fringe noise reduction is obtained. Fitting of the spectrum with fringe-reduction is shown (black line) and SNR of 452 was achieved (calculated as amplitude of the fit divided by the standard deviation of the data measured away from the NO transition).

These AOM temperature variations result in fringe reduction by  $\sim 16$  times. The total noise measured was reduced from 340 Hz before to 41 Hz after the fringe-reduction technique was applied. The total gas pressure of 8.99 Torr and the NO concentration of 1124 ppm were retrieved by fitting the fringe-free data. Although fitting of the data with fringes is also possible, performing the fringe reduction has two advantages: (i) some essential features of the signal may be interfered by fringes thus the confidence of the fitting is higher after fringe reduction and (ii) lack of fringes allows for simplification of the fitting process, especially when one of the parameters is known (e.g. when pressure is known measurement of the amplitude might be enough to determine the concentration without the fitting process, which is time consuming). SNR observed in the dispersion spectrum after the fringe-reduction is 452, which correspond to a minimum detection limit of 0.39 ppm for 1 m pathlength and 1 s averaging time. This result is consistent with the value predicted by the SNR simulation shown in Fig. 3b if we take into account that: 1) fringes were not removed fully, 2) we have used a different chirp rate (higher chirp rates give better results when fringes are only partially removed), and 3) there were different gas pressures used in the two presented experiments (in dual-frequency CLaDS that is presented in this paper, pressure-broadening of the absorption line affects the amplitude of the CLaDS signal measured at a fixed AOM frequency shift).

#### *Impact of the beatnote power on noise*

As mentioned in previous sections, the amplitude of the dispersion signal does not depend on optical power, thus it is highly immune to changes of the total detected laser power. This property of CLaDS was demonstrated in Ref. [8, 11]. Noise, however, has a slight dependence on the power of the beatnote. The noise in the FM-demodulated signal increases when the carrier to noise ratio (CNR) is decreased but as long as the CNR is above a certain level required for accurate FM demodulation the effect on the observed SNR is very small [9]. To explore how change of the CNR level affects the SNR in CLaDS the noise was measured at different powers of the heterodyne beatnote, ranging from 0dBm to -30dBm. Four spectral scans performed at different power levels far away from the molecular transition are shown in Fig. 5.

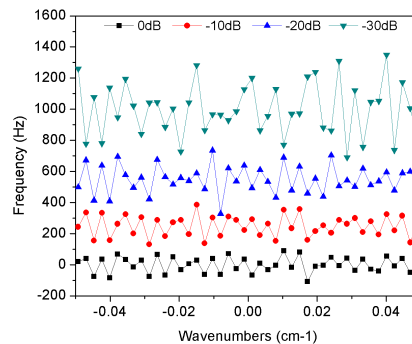


Figure 5. CLaDS dispersion spectra measured away from molecular transition acquired at different RF powers of the heterodyne beatnote (spectra are offset in y-axis for clarity).

The measurement in Fig. 5 were acquired in similar conditions as previously used (chirp rate = 420 kHz/ns,  $BW = 5$  MHz, 10000 consecutive scans averaged). The observed noise is below 50 Hz for heterodyne power level of 0 dBm and increases by 1.3 dB, 2.5 dB and 5.4 dB for RF powers of -10 dBm, -20 dBm and -30 dBm respectively. Only small ( $< 3$ dB) deterioration of the SNR is observed when the CNR is reduced by more than 20 dB. The minimum detection limit stays below 1 ppm (for 1 m pathlength and 1 s averaging time) even when the RF beatnote power is decreased by  $\sim 30$  dB. At the same time signal amplitude remains unaffected (as shown in Ref. [8, 11]). These properties enable utilization of low-cost retroreflectors or natural topographic targets for back-scattered/reflected light detection and prove the suitability of CLaDS for remote long-distance and open-path sensing applications.

## 4. CONCLUSIONS

In this paper an optical heterodyne detection-based spectroscopy method was described. The theoretical background of CLaDS and its suitability for remote detection was introduced. The CLaDS signal and noise performance were analyzed experimentally using a mid-IR QCL targeting the transition at  $1906.7 \text{ cm}^{-1}$  in the fundamental ro-vibrational band of nitric oxide around  $5.2 \mu\text{m}$ . We have found that fringes are the main limitation of the minimum detection limit in the presented system. A technique of fringe removal based on randomization of the parasitic etalon pattern followed by a

subsequent averaging enables significant SNR improvement and allows for ultra-sensitive NO sensing. The impact of the heterodyne beatnote power on CLaDS noise performance was analyzed. It was shown that since the dispersion signal in CLaDS is retrieved using frequency demodulation, the reduction of the beatnote (carrier) power level has small impact on the SNR. This feature of CLaDS makes it well suited for open-path remote sensing of chemical traces even in environments that show high transmission fluctuations (i.e. due to particulate matter or turbulence).

### ACKNOWLEDGEMENT

Funding for the work was provided by the NSF through the CAREER award CMMI-0954897 and in part from the MIRTHE NSF Engineering Research Center.

### REFERENCES

- [1] Faist, J., Capasso, F., Sivco, D. L., Sirtori, C., Hutchinson, A. L. and Cho, A. Y., "Quantum Cascade Laser," *Science* 264, 553-556 (1994).
- [2] Curl, R. F., Capasso, F., Gmachl, C., Kosterev, A. A., McManus, B., Lewicki, R., Pusharsky, M., Wysocki, G. and Tittel, F. K., "Quantum cascade lasers in chemical physics," *Chemical Physics Letters* 487, 1-18 (2010).
- [3] Duxbury, G., Langford, N., McCulloch, M. T. and Wright, S., "Quantum cascade semiconductor infrared and far-infrared lasers: from trace gas sensing to non-linear optics," *Chemical Society Reviews* 34, 921-934 (2005).
- [4] Kosterev, A. A. and Tittel, F. K., "Chemical sensors based on quantum cascade lasers," *Quantum Electronics, IEEE Journal of* 38, 582-591 (2002).
- [5] McManus, J. B., Nelson, D. D., Herndon, S. C., Shorter, J. H., Zahniser, M. S., Blaser, S., Hvozدارa, L., Muller, A., Giovannini, M. and Faist, J., "Comparison of cw and pulsed operation with a TE-cooled quantum cascade infrared laser for detection of nitric oxide at  $1900\text{ cm}^{-1}$ ," *Applied Physics B: Lasers and Optics* 85, 235-241 (2006).
- [6] Available: [www.cascadestech.com](http://www.cascadestech.com)
- [7] Taslakov, M., Simeonov, V., Froidevaux, M. and van den Bergh, H., "Open-path ozone detection by quantum-cascade laser," *Applied Physics B: Lasers & Optics* 82, 501-506 (2006).
- [8] Wysocki, G. and Weidmann, D., "Molecular dispersion spectroscopy for chemical sensing using chirped mid-infrared quantum cascade laser," *Opt. Express* 18, 26123-26140 (2010).
- [9] Silver, J. A. and Slanton, A. C., "Optical interference fringe reduction in laser absorption experiments," *Appl. Opt.* 27, 1914-1916 (1988).
- [10] Franz, K., Weidmann, D. and Wysocki, G., "High Dynamic Range Laser Dispersion Spectroscopy of Saturated Absorption Lines," *Conference on Lasers and Electro-Optics CMJ4* (2010).